A Novel b-shaped L-type Transformerless Hybrid Active Power Filter in Three-Phase Four-Wire Systems

Chi-Seng Lam, *Student Member, IEEE*, and Man-Chung Wong, *Member, IEEE*

***Abstract*—This paper presents a novel b-shaped L-type transformerless hybrid active power filter (HAPF) for reactive power, current harmonics and neutral current compensation in three-phase four-wire distribution power system. The passive filter (PF) is tuned to compensate the dominant harmonic current and also reactive power of the load, while the active power filter (APF) compensates the remaining harmonic and reactive power values. With appropriate design of the system parameters, the novel HAPF topology can prevent most of the fundamental voltage and current across the APF. This results in a great reduction of the APF's VA rating, but without significantly deteriorates the system compensation capability. Moreover, transformerless HAPF benefits by eliminating the transformer phase shift, voltage drop, harmonics loss, bulky size and expensive cost. As a result, the proposed HAPF is characterized by small APF capacity, economical cost, well filtering effect and easy realization. And it is suitable to be implemented in high voltage and current conditions. A DC-link power flow controller is also employed to uniform its voltage level. Finally, simulation results are given to verify the viability and effectiveness of the novel HAPF.**

***Index Terms*—Power electronics, power quality.**

I. Introduction

According to the proliferation and development of power electronics equipments (nonlinear loads) in automatic production line, computer centre, hospital, etc; their processes inject a large amount of harmonic currents into the utility power system [1]–[5], and thus increase the overall reactive power demanded by the load. Harmonic distortion may also cause equipment overheating, capacitor fuse blowing, etc [3]. In order to eliminate the harmonic currents, filtering device is needed to place between the load and the source side.

Since the first installation of a passive tuned filter in the mid 1940's, the use of filters to solve current quality problems has been an area of continuing research [6]. Passive filters (PFs) consist of a bank of tuned *LC* filters and/or a high-pass filter have been widely used to suppress harmonics and improve power factor due to its low initial cost, simplicity and high efficiency [1]–[4], [7], [8]. These filters however have inherent drawbacks:

1) Source impedance strongly affects filtering characteristics [1]–[4], [7].
2) The shunt PF may fall in series resonance with the source impedance [1]–[4], [7].
3) A harmonic amplifying phenomenon occurs due to parallel resonance between the source line inductance and PF capacitance [1]–[4].
4) Small variations in the values of L or C modify the filter resonant frequency and filtering characteristics [3], [7].
5) The PF generates fundamental frequency reactive power, over-voltage can be generated at its terminals during low load operating conditions [7].

Since the concept "Active ac Power Filter" was first developed by L. Gyugyi in 1976 [6], the research studies of the active power filters (APFs) for current quality compensation are prospering since then. In addition, the APFs have the ability to overcome the above mentioned drawbacks inherent in PFs. However, the initial costs and running costs of the APFs are much higher than the PFs [1]–[4], [9].

In order to lower the rating and cost of the APFs, hybrid filter structure will be a good choice. Hybrid active power filters (HAPFs) consists of active and passive filters connected in series or parallel with each other and there are mainly two advantages:

1) The resonance of PF with system inductance can be prevented [1]–[4], [7], [8].
2) The rating of the APF can be reduced so as to reduce the cost of the whole system [1]–[8].

Some researches also pointed out that HAPF leads to the best effectiveness in cost and performance in the current quality compensation [1]–[2], [10]. Hereinafter, the two general HAPF topologies are shown in Fig. 1 and their APF's required ratings are summarized in Table I. Since the series connection offers stronger potential for reduced APF rating, Fig. 1 (b) topology is preferable.

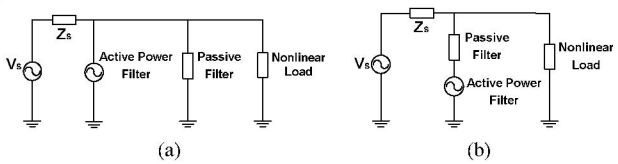

Fig. 1. Two general HAPF topologies: (a) PF and APF connected in parallel, (b) PF and APF connected in series.

This work has been financially supported by the *Science and Technology Development Fund, Macao SAR Government.*

C.-S. Lam and M.-C. Wong are with the Faculty of Science and Technology, University of Macau, Macao, SAR, P. R. China (e-mail: C.S.Lam@ieee.org; mcwong@umac.mo). 1-4244-0228-X/06/$20.00 ©2006 IEEE

TABLE I
APF'S REQUIRED RATINGS FOR TWO GENERAL HAPF TOPOLOGIES

	PF and APF connected in parallel [1]–[3], [6]	PF and APF connected in series [3]–[8], [10]–[11]
APF's voltage & current ratings	Rather High	Potentially Low

In this paper, the HAPF for three-phase four-wire power system will be the main concern, so that neutral current can also be compensated. For the HAPF adopted in distribution site, transformerless-coupled structure is appreciated by eliminating the transformer phase shift, voltage drop, harmonics loss, bulky size, and expensive cost. Furthermore, the rating of the APF is actually not being changed by the coupling transformer [1], [10].

In order to further reduce the APF current rating in Fig. 1 (b), an additional passive branch can be added parallel to the APF [6], [9], so as to reduce the fundamental current across the APF. Moreover, PF can still operate normally even if the APF is broken. Fig. 2 shows four possible transformerless HAPF topologies and Table II illustrates their comparisons.

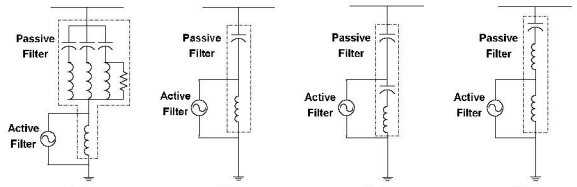

Fig. 2. Four possible transformerless HAPF topologies: (a) multi-branch passive filter, (b) b-shaped one-branch passive filter, (c) b-shaped C type [11], (d) proposed b-shaped L-type.

TABLE II
COMPARISONS OF FOUR POSSIBLE TRANSFORMERLESS HAPF TOPOLOGIES

Topologies	(a)	(b)	(c)	(d)
Size	Largest	Smallest	Medium	Small
Initial cost	Largest	Smallest	Medium	Small
Switching noise injection	Small	Large	Large	Smallest

A multi-branch PF is used in Fig. 2 (a). According to the main harmonic components in the load current, multi-branch PF with different resonant frequencies can be chosen. However, the multi-branch PF increases the cost and volume of the whole filter. Since the APF has the ability to filter the remained harmonics, the number of PF branches can be reduced.

In order to reduce the size and initial cost of the HAPF, Fig. 2 (b) uses only one-branch PF. This topology has the minimum volume. However, the switching noise flows into the main system through the capacitor if no extra output filter is added.

Another topology named "C type" HAPF [11] is shown in Fig. 2 (c). The lower capacitor resonates with the inductor at the fundamental frequency. Therefore, the fundamental frequency current does not flow into the APF. Even though the APF required rating can be greatly reduced, large ac capacitances are required. The large ac capacitance increases the cost and volume of the HAPF. Moreover, this topology still involves the switching noise problem as Fig. 2 (b).

Fig. 2 (d) shows the proposed b-shaped L-type transformerless HAPF topology. The upper inductor can damp the switching frequency ripples, which solve the switching noise problem in Figs. 2 (b) and (c). Since the filtering inductors are usually in small values, most of the fundamental and dominant load harmonic currents do not flow into the APF. As a result, this topology can effectively damp the switching noise, obtain both small APF rating and PF's volume, thus being chosen in this paper.

For the APF configuration in the proposed HAPF, 2-level four-leg inverter is chosen. Compared with center-split inverter, it although slightly increases the number of switches but is outweighed by a lower DC-link rating [12], and a higher neutral current compensation capability [13]. In this paper, an analysis of the proposed novel HAPF system parameters in the compensation performance is presented. A formula estimating the VA rating of the APF is given. A DC-link power controller is also employed to uniform its voltage level. Finally, simulation results are presented to illustrate the compensation characteristics, and the APF's required rating of the proposed HAPF topology.

II. PROPOSED NOVEL B-SHAPED L-TYPE TRANSFORMERLESS HAPF IN THREE-PHASE FOUR-WIRE POWER SYSTEM

Fig. 3 shows the proposed novel three-phase four-wire b-shaped L-type transformerless HAPF circuit configuration. It is named "b-shaped L-type" due to the PF and APF connection shape, and the extra inductor of the PF. The system is installed in parallel with nonlinear load. If h_n and h_{n1} are the most and second most dominant harmonic orders in load current, the filtering capacitance C_1 and inductance L_1 will have a resonance at h_{n1} harmonic order frequency, while the PF (C_1 , L_1 and L_2) will have a series resonance at h_n harmonic order frequency. In addition, the reactive power can be compensated by C_1 . The C_1 value respects to different load capacity, current total harmonic distortion and power angle can be chosen via [14]. Once C_1 and resonant frequencies $h_n\omega_f$ and $h_{n1}\omega_f$ (ω_f is the fundamental frequency) are determined, the filtering inductances L_1 and L_2 can be known. From Fig. 3, the PF can be operated itself or together with the APF by controlling the switches SW_P and SW_A.

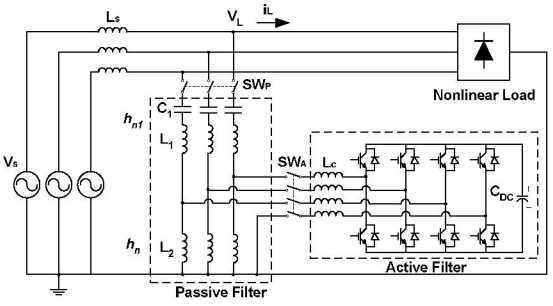

Fig. 3. Configuration of the proposed novel three-phase four-wire b-shaped L-type transformerless HAPF.

Provided that the APF of the proposed novel HAPF is controlled as current controlled current source:

$$i_{APF} = K_1 i_{qf} + K_2 i_{sh} \quad (1)$$

where K_1, K_2 are the gains for i_{qf}, i_{sh}, i_{qf} and i_{sh} are the fundamental reactive power and harmonic contents of the source current. Fig. 4 shows a single-phase equivalent circuit of the proposed novel HAPF. Based on Fig. 4, its study and analysis will be introduced.

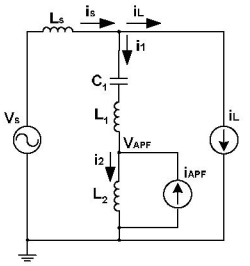

Fig. 4. A single-phase equivalent circuit of the proposed novel b-shaped L-type transformerless HAPF.

A. Analysis of the Novel b-shaped L-type Transformerless HAPF at fundamental frequency

Fig. 5 shows a single-phase equivalent circuit of the proposed novel HAPF at the fundamental frequency, where $i_{APFf} = K_1 i_{qf}$. Z_{sf}, Z_{1f} and Z_{2f} are the source impedance, filtering impedances of the PF at the fundamental frequency, V_{sf} is the fundamental voltage components in supply source. From Fig. 5, the effective fundamental voltage across the APF can be expressed as:

$$V_{APFf} = \frac{Z_{2f}(V_{sf} + K_1 i_{qf} Z_{1f} + K_1 i_{qf} Z_{sf} - i_{Lf} Z_{sf})}{Z_{sf} + Z_{1f} + Z_{2f}} \quad (2)$$

It is assumed that the fundamental source impedance Z_{sf} is very small ($Z_{sf} \approx 0$), simplify (2) yields,

$$V_{APFf} = \frac{V_{sf}}{Z_{1f}/Z_{2f} + 1} + \frac{K_1 i_{qf}}{1/Z_{1f} + 1/Z_{2f}} \quad (3)$$

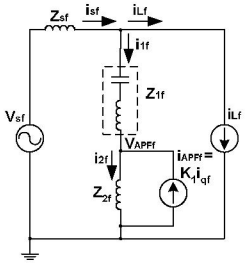

Fig. 5. A single-phase equivalent circuit of the proposed novel HAPF at the fundamental frequency.

Since Z_{2f} is usually small comparing with Z_{1f} ($Z_{1f} >> Z_{2f}$), thus Z_{1f} dominates the first term of (3), while Z_{2f} dominates the second term. From the first term of (3), the fundamental component of the source voltage is almost blocked by Z_{1f}, the APF fundamental voltage includes only small part of the source voltage. As a result, the required VA rating of the APF at the fundamental frequency can be reduced significantly if $K_1 i_{qf}$ is not large.

B. Analysis of the Novel b-shaped L-type Transformerless HAPF at harmonic frequency

Considering the compensation of the harmonic contents of the load current, Fig. 6 shows a single-phase HAPF equivalent circuit at the harmonic frequency, where $i_{APFh} = K_2 i_{sh}$. The nonlinear load is considered as a harmonic current source. Z_{sh}, Z_{1h} and Z_{2h} are the source impedance, filtering impedances of the PF at the harmonic frequency, V_{sh} is the harmonic voltage components in supply source. From Fig. 6, the source harmonic current i_{sh} is:

$$i_{sh} = \frac{V_{sh} + (Z_{1h} + Z_{2h}) i_{Lh}}{Z_{sh} + Z_{1h} + (1 + K_2) Z_{2h}} \quad (4)$$

For simplicity, the source voltage V_s is being assumed to have no harmonic components (V_{sh}=0), (4) yields,

$$i_{sh} = \frac{(Z_{1h} + Z_{2h}) i_{Lh}}{Z_{sh} + Z_{1h} + (1 + K_2) Z_{2h}} \quad (5)$$

From (5), the source harmonic current i_{sh} can be reduced greatly when Z_{1h} and Z_{2h} are close to zero. Increasing K_2 value can also improve the filtering performance, but the value of K_2 has limitation due to the stability problem. The resonance will not occur even if $|Z_{sh} + Z_{1h}| \approx 0$ due to the term of $(1 + K_2) Z_{2h}$ in the denominator of (5). Under the ideal filtering performance i_{sh}=0, the harmonic voltage across the APF equals the harmonic voltage drop on Z_{1h}, which is given as:

$$V_{APFh} = i_{Lh} Z_{1h} \quad (6)$$

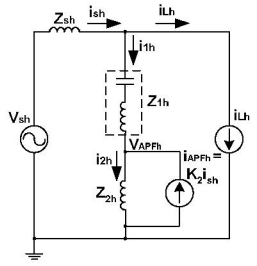

Fig. 6. A single-phase equivalent circuit of the proposed novel HAPF at the harmonic frequency.

And the harmonic current across the APF can be determined as $K_2\, i_{sh}$ (1).

C. Stability & APF Rating Analysis of the Novel b-shaped L-type Transformerless HAPF

Based in the Laplace transformation, $Z_s = sL_s$, $Z_{C1} = 1/sC_1$, $Z_{L1} = sL_1$, $Z_{L2} = sL_2$,

$$\frac{I_s(s)}{I_L(s)} = \frac{s^2 C_1(L_1 + L_2) + 1}{s^2[C_1(L_1 + L_s) + (1 + K_2)L_2C_1] + 1} \tag{7}$$

By ROUTH-HURWITZ criterion, the Routh table can be obtained. In order to have good stability for the HAPF system, $K_2 > 0$, but the value of K_2 has limitation due to the stability problem.

The VA rating of the APF in the proposed HAPF is:

$$VA_{APF} = 3V_{APF} i_{APF} = 3(V_{APFf} + V_{APFh}) \times (i_{APFf} + i_{APFh}) \tag{8}$$

$$VA_{APF} = 3\left(\frac{V_{sf}}{Z_{1f} \,/\!/\, Z_{2f} + 1} + \frac{K_1 i_{qf}}{1/Z_{1f} + 1/Z_{2f}} + i_{Lh} Z_{1h}\right) \times (K_1 i_{qf} + K_2\, i_{sh}) \tag{9}$$

For calculation simplicity, it is assumed that both the branch C_1 and L_1 impedance at the dominant harmonic frequency and the other harmonic values are small, i.e. $i_{Lh} Z_{1h} \approx 0$, $V_{APFh} \approx 0$, (9) can be simplified as:

$$VA_{APF} = 3\left(\frac{V_{sf}}{Z_{1f} \,/\!/\, Z_{2f} + 1} + \frac{K_1 i_{qf}}{1/Z_{1f} + 1/Z_{2f}}\right) \times (K_1 i_{qf} + K_2\, i_{sh}) \tag{10}$$

The ratio of the VA rating of the APF over that of the load for both single-phase and three-phase system can be estimated by:

$$\frac{VA_{APF}}{VA_{Load}} = \frac{3\left(\frac{V_{sf}}{Z_{1f} \,/\!/\, Z_{2f} + 1} + \frac{K_1 i_{qf}}{1/Z_{1f} + 1/Z_{2f}}\right) \times (K_1 i_{qf} + K_2\, i_{sh})}{3V_{sf} \times i_L} \tag{11}$$

Since Z_{2f} is usually small comparing with Z_{1f} , also $i_L >> i_{qf}$ and $i_L >> i_{sh}$, the VA rating of the APF can be reduced significantly if K_1 and K_2 are not large and estimated by (10).

D. Control of DC-link Power in the Novel b-shaped L-type Transformerless HAPF

During HAPF operation, if the integration of the DC storage capacitor power P_{dc} within a period of time is not zero, the DC-link voltage will have variations.

$$\int_{t_0}^{t} P_{dc}(\tau)\, d\tau = \frac{C_{dc}}{2}\left[V_{dc}^2(t) - V_{dc}^2(t_0)\right] \tag{12}$$

where C_{dc} represents the DC storage capacitance, $V_{dc}(t)$ represents the DC capacitor voltage after a period of $t - t_0$, $V_{dc}(t_0)$ represents the initial DC capacitor voltage. In order to maintain a uniform DC-link voltage, its power should be controlled so that P_{dc} over a period of time equals zero. In the following, the control of DC-link power and its detection method will be introduced.

Fig. 7 shows the HAPF DC storage active power control block diagram. First of all, the source instantaneous active power P_s is being calculated using the instantaneous power theory [15]–[17], where $D_{HP}(s)$ is the high-pass filter used in extracting the AC component (source harmonic contents) $\tilde{P}_s$ of P_s . The reference active power change of the APF is obtained by the addition of DC component $\overline{P}_{dc\_comp}$ and subtraction of AC component $\tilde{P}_s$. P_{dc} is the addition of P_{APF} and the subtraction of power loss P_{Loss} . If the APF can output the calculated reference current without error, it can be viewed as a unity gain block in Fig. 7. In order to control P_{dc} such that the DC-link voltage is uniform, a PI feedback path is added. When the DC capacitor absorbs in excess of active power, the value of $\overline{P}_{dc\_comp}$ should be lowered to prevent the DC-link voltage level rise, and vice versa.

From Fig. 7, P_{dc} can be expressed as (13):

$$P_{dc}(s) = \frac{s^2[-P_L(s)D_{HP}(s)]}{s^2[1 - D_{HP}(s)] + sK_p + K_I} + \frac{s^2[P_{PF}(s)D_{HP}(s)]}{s^2[1 - D_{HP}(s)] + sK_p + K_I} + \frac{s^2[-P_{Loss}(s)(1 - D_{HP}(s))]}{s^2[1 - D_{HP}(s)] + sK_p + K_I} \tag{13}$$

From (13), P_{dc} is affected by three inputs: load power P_L , passive filter power P_{PF} and power loss P_{Loss} . The steady-state P_{dc} value with respect to the three inputs is found to be zero. Since they have no effect on P_{dc} in steady-state, that is $\overline{P}_{dc} = 0$, thus the DC-link voltage can be kept uniform after a PI feedback path is added.

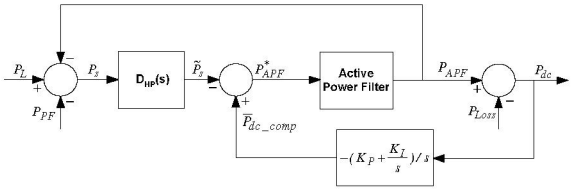

Fig. 7. HAPF DC storage active power control block diagram

Since there are high switching frequency components in the detection of DC storage power, there will be error if the numerical integration is done by digital controller. As indicated by (12), the integration of the DC storage power can be replaced by the detection of instantaneous DC voltage value, instead of the more complicated numerical integration method. By applying PI controller for the DC capacitor power P_{dc}, it can achieve zero value in steady-state. Thus, the DC-link voltage can be maintained uniform.

E. Control Block Diagram of the Novel b-shaped L-type Transformerless HAPF

For setting the APF's gains K_1 and K_2 equal 1, the instantaneous power theory [15]–[17] is applied for the APF operation. Fig. 8 shows a control block diagram of the proposed novel HAPF with DC-link power control consideration. For the PF, it compensates the most dominant load harmonic current and reactive power, while the remaining harmonic and reactive power values are compensated by the APF. For the APF, first of all, the source voltage V_s, source current i_s, compensating current i_c and DC-link voltage V_{dc} are sampled with a fixed frequency of 10kHz. The measured DC-link voltage V_{dc} and the reference V_{dc}^* after some mathematical calculations are then fed into a PI controller, which yields $\overline{P}_{dc\_comp}$, the DC-link variation compensating power. After calculation of the instantaneous source power, the source reactive power q_s and oscillating power $\tilde{P}_s$ are then added together with $\overline{P}_{dc\_comp}$ for reference compensating current i_c^* calculation. Subtracting the compensating current i_c from i_c^* yields the compensating current error Δi_c. The PWM switching signals are determined by comparing Δi_c with a hysteresis band ($\pm H$). The aim is to keep the current error Δi_c remains inside the error band. Hysteresis PWM control is also applied for the neutral line current compensation.

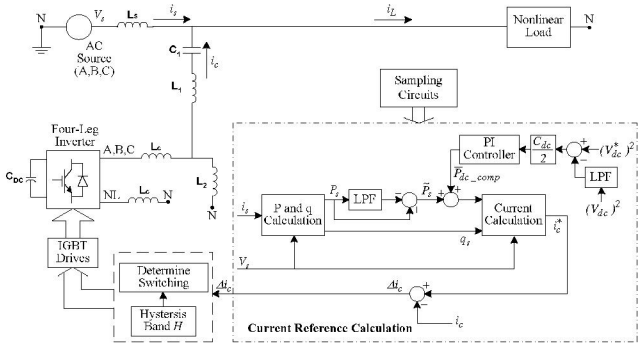

Fig. 8. Control block diagram of the proposed novel HAPF with DC-link power control consideration.

III. Simulation Results

In this section, representative simulation results are included to illustrate and verify the compensation performances of the proposed HAPF. The system configuration is shown in Fig. 1. The simulation studies have been carried out using PSCAD/EMTDC. For setting K_p =10 and K_I =0.035 in PI controller, Table III shows an 110V/1.65kVA novel HAPF system parameters for simulations, in which the PF is tuned at the dominant 3rd harmonic order frequency while the branch L_1 and C_1 is tuned at 5th harmonic order frequency.

TABLE III
AN 110V/1.65KVA NOVEL HAPF SYSTEM PARAMETERS

Test Parameters	Nominal Values
V_s	110V_{rms}/50Hz
Source inductance L_s	1.0mH
Filtering inductance L_1	5.3mH
Filtering capacitance C_1	76.0μF
Filtering inductance L_2	9.5mH
Inverter inductance L_c	20.0mH
DC storage capacitance C_{dc}	10mF (Initial charge to 100VDC)
Nonlinear load (balanced)	5.2A_{rms} (Power Factor =0.85)
Switching frequency f_s	10kHz

Fig. 9 (a) shows three-phase load current and neutral current waveforms before compensation. In which, the compensated source current and neutral current waveforms with only PF and the novel HAPF operations are illustrated in Figs. 9 (b) and (c) respectively. Moreover, Fig. 10 shows the frequency spectra of the source currents and neutral current before and after

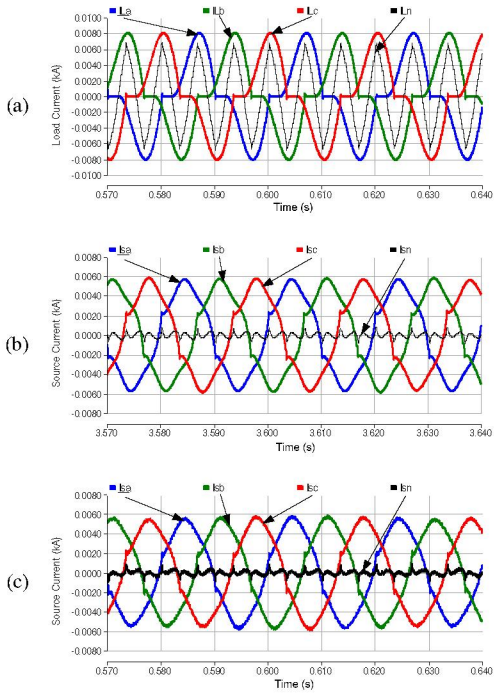

Fig. 9. (a) Three-phase load currents and neutral current, (b) source currents and neutral current with only PF operation, (c) source currents and neutral current with the novel HAPF operation.

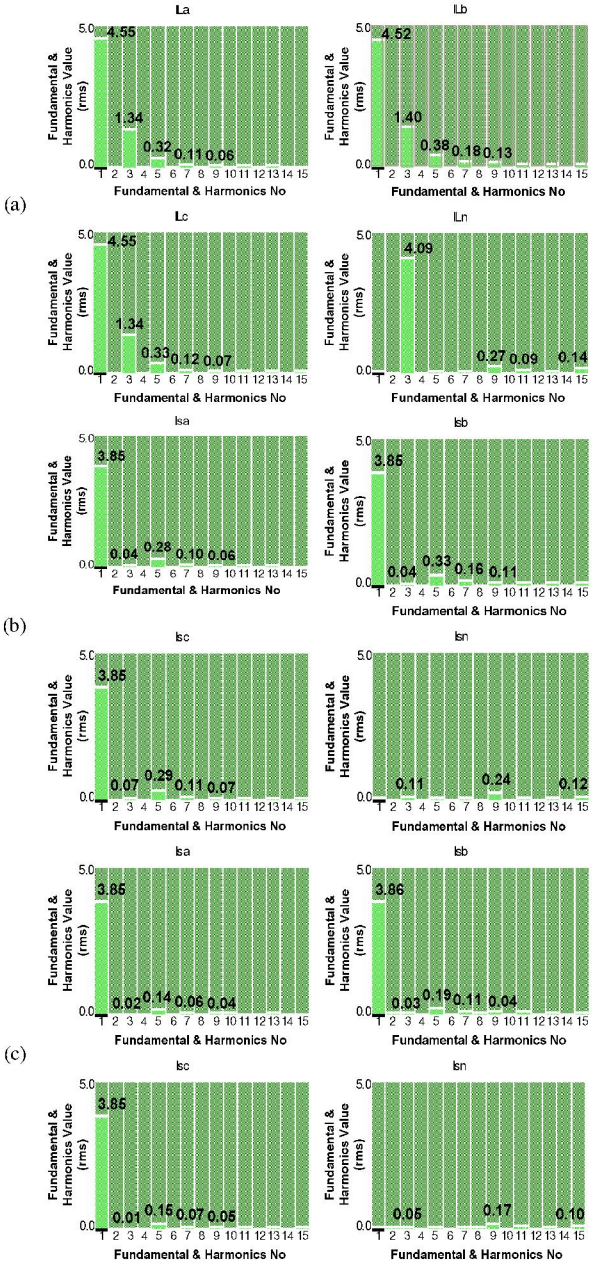

Fig. 10. Frequency spectra: (a) three-phase load currents and neutral current, (b) source currents and neutral current with only PF operation, (c) source currents and neutral current with the novel HAPF operation.

compensations. From Fig. 10 (a), there are odd harmonics occurring at load and neutral currents, and the 3rd harmonic component dominates those harmonic currents. With pure PF operation case, since the PF is tuned at the dominant 3rd harmonic order frequency, it can eliminate the 3rd harmonic load and neutral currents, as shown in Fig. 10 (b). For the novel HAPF operation, besides the 3rd harmonic currents elimination by PF, its active part can compensate higher order harmonic currents, thus further improves the harmonic filtering performance, as shown in Figs. 9 (c) and 10 (c). From Fig. 10 (c), there are little even harmonics generated to the system due to the unsymmetrical switching frequency of the APF. From both Figs.

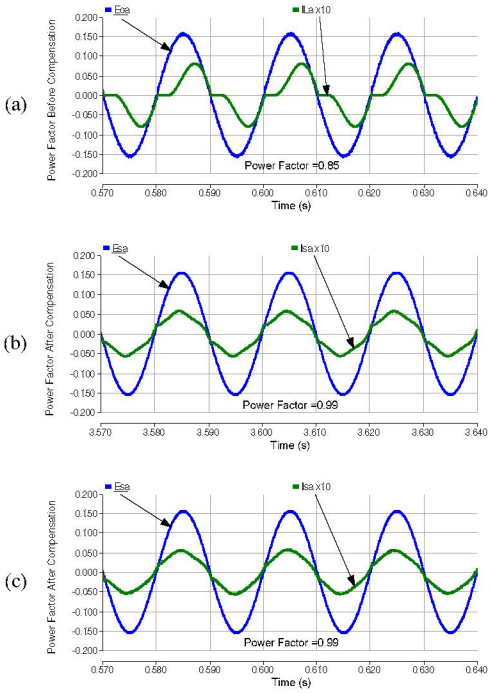

Fig. 11. Power factor (Phase A): (a) before compensation, (b) after PF compensation, (c) after HAPF compensation.

9 and 10, the proposed novel HAPF can effectively suppress the harmonic components of nonlinear load currents and compensate the neutral current. These simulation results show the effect of compensation over oscillating source active and reactive power $\tilde{p}_s$ and $\tilde{q}_s$.

Fig. 11 shows that the reactive power can be compensated simultaneously with the current harmonics and neutral current as well. The compensation of the reactive power results in increasing the power factor. This part clearly shows the effect of compensation over average source reactive power $\overline{q}_s$. It can be seen from Fig. 11 (b) and (c) that phase A source current and voltage become almost in-phase after compensation. Compared with Fig. 11 (a), the power factor has been improved from 0.85 to 0.99, which shows the effectiveness of power factor correction using the PF and the novel HAPF compensations.

After the implementation of the DC-link power controller in the novel HAPF, its voltage level can be kept at its reference level (100V), as shown in Fig. 12 (a). From Fig. 12 (b), there is little current across the APF through phase A, that is 0.70A_{rms}. Moreover, the APF's phase A operating voltage is 20.2V_{rms}. Thus, the VA rating of the APF is merely 2.4% of the harmonic-producing load, which is consistent with (11). As a result, the APF rating in the proposed novel HAPF can be proved to reduce greatly and estimated by (10).

Finally, Table IV summarizes phase A (same with B and C) and neutral current compensation performance before and after the PF and the novel HAPF operations. Phase A total harmonic distortion (THD) of the load current, input power factor and neutral current before compensation are 30%, 0.85 and 4.0A_{rms}

respectively. During pure PF operation, phase A THD of the source current, input power factor and source neutral current have been improved to 8.9%, 0.99 and 0.28A_{rms}. When the novel HAPF is operating, those compensation parameters can be further improved to 5.3%, 0.99 and 0.19A_{rms}. Moreover, the APF's phase A operating voltage and current are merely 20.2V_{rms} and 0.70A_{rms} respectively. Consequently, from the summarizations in Table IV, the proposed novel HAPF system can obtain well compensation performances with small APF capacity.

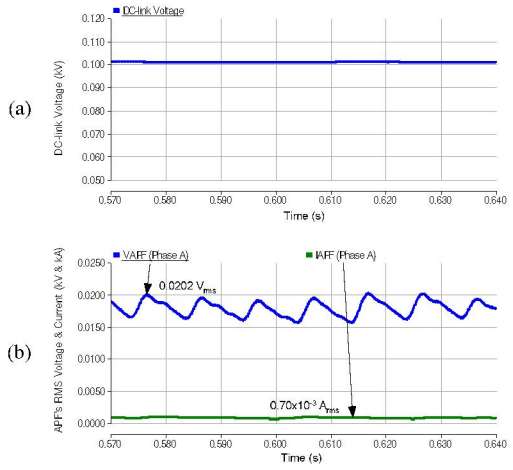

Fig. 12. Hybrid active power filter (HAPF): (a) DC-link voltage, (b) APF's phase A operating voltage and current.

TABLE IV
SUMMARIZES PHASE A AND NEUTRAL CURRENT COMPENSATION PERFORMANCE BEFORE AND AFTER PF AND THE NOVEL HAPF OPERATION

	No Filter	PF	HAPF
Phase A THD of Source Current i_{sa}	30%	8.9 %	5.3 %
Phase A Input Power Factor	0.85	0.99	0.99
Source Neutral Current RMS i_{sn}	4.0A_{rms}	0.28A_{rms}	0.19A_{rms}
APF's phase A operating voltage			20.2V_{rms}
APF's phase A operating current			0.70A_{rms}

IV. CONCLUSION

In this paper, a novel b-shaped L-type transformerless HAPF for reactive power, current harmonics and neutral current compensation in three-phase four-wire power system is proposed. The proposed HAPF topology can greatly reduce the VA rating of the APF, but without significantly deteriorate the compensation capability. Another advantage of the proposed topology is that the PF can normally operate by itself if the APF is broken. An analytical investigation of the proposed HAPF characteristics, filtering performances and VA rating of the APF are performed. And a DC-link power controller is also employed for the HAPF to compensate the inverter losses and uniform the DC-link voltage level. Finally, simulation results verify the viability and effectiveness of the proposed HAPF topology. And the proposed novel HAPF is distinguished by small APF capacity, economical cost, well filtering effect and easy realization.

REFERENCES

[1] H. Fujita, and H. Akagi, "A practical approach to harmonic compensation in power systems – series connection of passive and active filters," *IEEE Trans. Ind. Applicat.*, vol: 27, pp. 1020–1025, Nov./Dec. 1991.

[2] F. Z. Peng, H. Akagi, and A. Nabae, "A new approach to harmonic compensation in power systems – a combined system of shunt passive and series active filters," *IEEE Trans. Ind. Applicat.*, vol: 26, pp. 983–990, Nov./Dec. 1990.

[3] L. Chen, and A. V. Jouanne, "A comparison and assessment of hybrid filter topologies and control algorithms," in *Proc. IEEE 32nd Annual Power Electronics Specialists Conf., PESC. 01*, vol: 2, 2001, pp. 565–570.

[4] S. Park, J.-H. Sung, and K. Nam, "A new parallel hybrid filter configuration minimizing active filter size," in *Proc. IEEE 30th Annual Power Electronics Specialists Conf., PESC. 99*, vol: 1, 1999, pp. 400–405.

[5] H. Akagi, S. Srianthumrong, and Y. Tamai, "Comparisons in circuit configuration and filtering performance between hybrid and pure shunt active filters," in *Conf. Rec. IEEE-IAS Annu. Meeting,* vol: 2, 2003, pp. 1195–1202.

[6] S. T. Senini, and P.J. Wolfs, "Systematic Identification and Review of Hybrid Active Filter Topologies," in *Proc. IEEE 33rd Annual Power Electronics Specialists Conf., PESC. 02*, vol: 1, 2002, pp. 394–399.

[7] D. Rivas, L. Moran, J.W. Dixon, et al., "Improving passive filter compensation performance with active techniques," *IEEE Trans. Ind. Electron.*, vol: 50, pp. 161–170, Feb. 2003.

[8] Y. Wang, Z. Wang, J. Yang, et al., "A new hybrid parallel active filter," in *Proc. IEEE 34th Annual Power Electronics Specialists Conf., PESC. 03*, vol: 3, 2003, pp. 1049–1054.

[9] H. Akagi, "New trends in active filters for power conditioning," *IEEE Trans. Ind. Appl.*, vol.32, pp.1312–1322, Nov./Dec. 1996.

[10] H. Fujita, T. Yamasaki, and H. Akagi, "A hybrid active filter for damping of harmonic resonance in industrial power systems," *IEEE Trans. Power Electron.*, vol: 15, pp.215–222, Mar. 2000.

[11] F. Liu, Y. P. Zhou, and H. Li, "The C type hybrid active power filter," in *Proc. of the CSEE*, vol: 25, 2005, pp.75–80.

[12] C. A. Quinn, N. Mohan, "Active filtering of harmonic currents in three-phase, four-wire systems with three-phase, single-phase nonlinear loads," in *Proc. IEEE APEC'92,* 1992, pp. 829–836.

[13] B. Singh, K. Al-Haddad, A. Chandra, "A review of active filters for power quality improvement," *IEEE Trans. Ind. Electron.,* vol: 46, pp. 960–971, Oct. 1999.

[14] G. J. Wakileh, "*Power systems harmonics*", Springer-Verlag Berlin Heidelberg, 2001.

[15] H. Akagi, Y. Kanazawa, and A. Nabae, "Instantaneous reactive power compensators comprising switching devices without energy storage components," *IEEE Trans. Ind. Aplicat.*, vol: 20, pp. 625–630, May/Jun. 1984.

[16] F. Z. Peng and J. S. Lai, "Generalized instantaneous reactive power theory for three-phase power systems," *IEEE Trans. Instrum. Meas.*, vol: 45, pp. 293–297, Feb. 1996.

[17] F. Z. Peng, G.W. Ott Jr, and D. J. Adams, "Harmonic and reactive power compensation based on the generalized instantaneous reactive theory for three-phase four-wire systems," *IEEE Trans. Power Electron.*, vol: 13, pp. 1174–1181, Nov. 1998.